Thermochimica Acta 520 (2011) 55–60

Contents lists available at ScienceDirect

Thermochimica Acta

journal homepage: www.elsevier.com/locate/tca

# Kinetic study of the redox process of iron oxide for hydrogen production at oxidation step

Fei Wen, Hui Wang*, Zongxun Tang

*Key Laboratory of Synthetic and Natural Functional Molecule Chemistry (Ministry of Education), College of Chemistry & Materials Science, Northwest University, Xi'an 710069, PR China*

ARTICLE INFO

*Article history:*
Received 3 December 2010
Received in revised form 9 March 2011
Accepted 14 March 2011
Available online 31 March 2011

*Keywords:*
Mo-Modified $Fe_2O_3$
Hydrogen production
Oxidation kinetics
Activation energy
Hydrothermal synthesis

ABSTRACT

Iron oxide ($Fe_2O_3$) is a potential substitute for other materials of hydrogen storage by a redox process of $Fe_3O_4$ (initial $Fe_2O_3$) + $4H_2 \leftrightarrow 3Fe + 4H_2O$ to store and release hydrogen. In order to evaluate the effectiveness of iron oxides with Mo additive for this purpose, the behaviors of unmodified and Mo-modified $Fe_2O_3$ samples ($Fe_2O_3$-none, $Fe_2O_3$–5%Mo, $Fe_2O_3$–8%Mo and $Fe_2O_3$–10%Mo), which were prepared by hydrothermal synthesis, were investigated for hydrogen production at oxidation step. Of all the samples, $Fe_2O_3$–8%Mo was the most effective for improving $H_2$ production at temperatures < 300 °C. The kinetic data at oxidation step obtained by isothermal experiments could be well fitted by the conventional and Jander equation. The apparent activation energy at oxidation step is about 55.53–65.30 kJ mol$^{-1}$ for unmodified $Fe_2O_3$ and about 36.17–45.19 kJ mol$^{-1}$ for $Fe_2O_3$–8%Mo based on the conventional and Jander models. The cooperative effect of active Fe and Mo additive on the $H_2O$ decomposition may be the main reason of lowering the activation energy.



## 1. Introduction

Utilization of hydrogen ($H_2$) as a transportation fuel is encouraged in the world because of increasing scarcity and cost of petroleum and urgent desire for abatement of air pollution [1,2]. However, one of the major obstacles to the use of hydrogen as an energy carrier is the lack of safe, efficient and low cost storage system [3,4]. Otsuka et al. proposed a promising alternative technology that can store and supply pure $H_2$ to PEFC vehicles by a simple reversible redox process of iron oxide [5–7], which can be simply described as $H_2$ storage (the reduction step 1: $Fe_2O_3 + 3H_2 \rightarrow 2Fe + 3H_2O$ or $Fe_3O_4 + 4H_2 \rightarrow 3Fe + 4H_2O$) and $H_2$ generation (the oxidation step 2: $3Fe + 4H_2O \rightarrow Fe_3O_4 + 4H_2$). In the redox process, a good cation-modified iron oxide sample prepared by urea method, which is also a potential alternative to other materials of storing hydrogen, can be recycled to use many times at a relatively low temperature. Based on this background, our group developed a simple, low cost method to prepare various cation-modified samples via impregnating iron or $Fe_2O_3$ powder with an aqueous solution containing corresponding metal cations [8,9]. It is found that the performances of the Mo-modified samples for $H_2$ production were significantly enhanced in the redox cycles, such as the catalytic activity and cyclic stability. In addition, the effect of Mo additive in the sample on improving hydrogen production was also investigated in our work. The result shows that the improvement of the catalytic activity and stability was attributed to the change of the Mo valence (Mo(III) ↔ Mo (IV)), namely, $MoO_2$ (initial $MoO_3$) was reduced by hydrogen to $Mo_2O_3$ in $H_2$ storage step and $Mo_2O_3$ was oxidized by water into $MoO_2$ again in the subsequent $H_2$ generation step. The change in the repeated redox cycles caused the variety of the sample structure, which suppressed the sintering of the sample particle [9]. In order to obtain an excellent modified sample as $H_2$ storage material that employs much lower $H_2$ production temperature (<300 °C) and much higher $H_2$ production rate (>250 μmol min$^{-1}$·Fe-g$^{-1}$) at < 300 °C in the oxidation step, the unmodified and several Mo-modified samples with different Mo amounts were synthesized by hydrothermal method.

At present, there have been some kinetic studies on the reduction step of modified and unmodified samples [3,10–13], but fewer kinetic studies on the oxidation step of the reduced samples in the redox process. In order to evaluate the suitability of different iron oxides as hydrogen storage material, the performances of the modified and unmodified samples for hydrogen production were investigated by the repeated redox cycles and the kinetic researches of the oxidation process were carried out by isothermal experiment at different operating temperatures.

* Corresponding author. Tel.: +86 029 88363115; fax: +86 029 88303798.
*E-mail address:* huiwang@nwu.edu.cn (H. Wang).

0040-6031/$ – see front matter © 2011 Elsevier B.V. All rights reserved.
doi:10.1016/j.tca.2011.03.015

## 2. Materials and methods

### 2.1. Sample preparation

Pure $Fe_2O_3$ and $Fe_2O_3$ with various amounts of Mo additive were prepared by hydrothermal synthesis: $Fe(NO_3)_3{\cdot}9H_2O$ (2.250 g) was dissolved in distilled water (10 ml) to form a clear solution, in which NaOH (2.8 M) was added to adjust the pH value until the Fe(3+) completely precipitated. The precipitate was filtered and washed with distilled water at 60 °C until the pH value of the filtrate reached 7 and followed by further decentralize in 20 ml distilled water with vigorous stirring to form the suspension liquid. After ultrasonic treatment for 30 min and stirring for 30 min, the suspension liquid added a certain amount of $(NH_4)_6Mo_7O_{24}{\cdot}4H_2O$ was transferred into Teflon-lined stainless-steel reactor with a capacity of 50 ml, followed by heating at 170 °C for hydrothermal treatment 2 h and subsequently cooled down to room temperature naturally. The hydrothermal product was washed by filter wash with distilled water and absolute ethanol, and then dried at 80 °C. The amount of the Mo additives was adjusted to 0. 5 mol%, 8 mol% and 10 mol% of the total metal cations (Mo/(Mo + Fe) = 0.00, 0.05, 0.08 or 0.10). The as-prepared samples were denoted as unmodified $Fe_2O_3$, $Fe_2O_3$–5%Mo, $Fe_2O_3$–8%Mo and $Fe_2O_3$–10%Mo.

### 2.2. Sample evaluation

The reaction apparatus used for the redox process of the samples is similar to that reported elsewhere [6]. The redox performances of these samples were evaluated by the WFSM-3012 evaluating device designed by ourselves. The procedure of increasing temperature of the reduction (step 1) and oxidation (step 2) of the samples was similar to the description in Ref. [7,8].

A set of isothermal oxidation experiments to produce hydrogen were carried out in the temperature range of 320–440 °C with a interval of 20 °C for each isothermal reaction in order to find the kinetic parameter for the oxidation of the reduced samples by water ($H_2O$) vapour. Dynamic experiments were conducted by the standard experimental conditions described as the previous report [8]. About 1.5 g of as-prepared sample was put into the reaction tube. The samples tested in this work was firstly reduced to active Fe by 1:1 gas mixture of $H_2$ and Ar with a flow rate of 40 ml $min^{-1}$ at 500 °C and subsequently oxidized to release hydrogen by 1:4 gas mixture of $H_2O$ vapor and Ar at given isothermal operating temperature. The amount of $H_2$ production was detected by on-line gas chromatography (GC). The reactivity of $H_2$ production of the Mo-modified and unmodified samples in the repeated redox cycles was evaluated by the following parameters: the rate of $H_2$ formation at temperatures below 300 or 300 °C, the temperature of $H_2$ formation at which the rate of $H_2$ formation is 250 μmol $min^{-1}{\cdot}Fe\text{-}g^{-1}$, the time of oxidation termination, the degree of oxidation of the reduced samples (DO), the amount of $H_2$ production and the activation energy in the oxidation step, i.e., the activation energy of $H_2$ production.

### 2.3. Data analysis

In the isothermal experiments the change of hydrogen production amount was registered as a function of time ($t$). The degree of oxidation of the reduced samples (DO) by $H_2O$ vapour was defined as the ratio of weight addition at any time to the total weight addition after complete oxidation, which corresponded to the ratio of hydrogen production amount at any time to the theoretical total hydrogen production amount after complete oxidation of the reduced sample (Fe) fed into reactor:

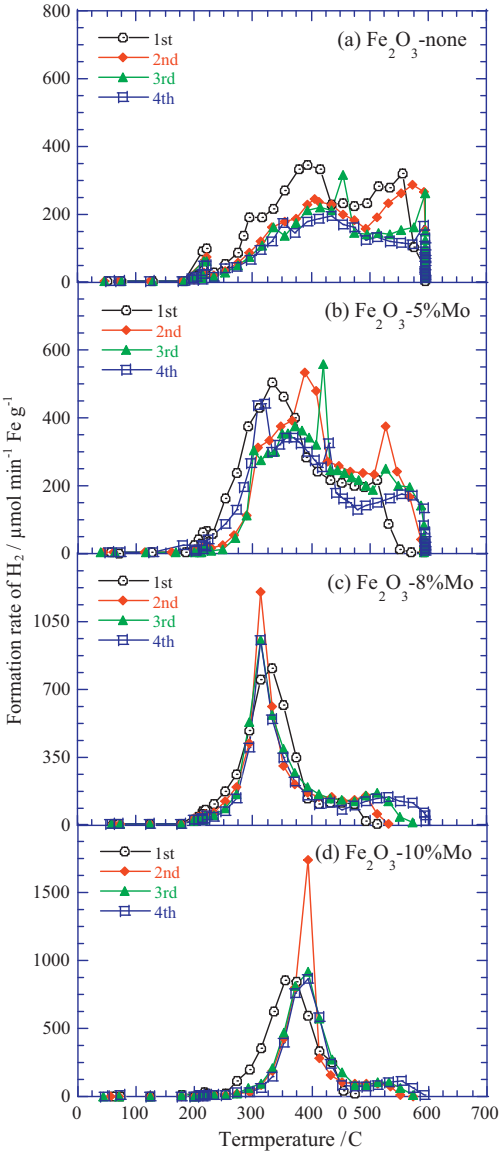


**Fig. 1.** Variations of formation rate of $H_2$ vs. temperature in the reoxidation of $Fe_2O_3$-none, $Fe_2O_3$–5%Mo, $Fe_2O_3$–8%Mo and $Fe_2O_3$–10%Mo in four repeated redox cycles.

$$\mathrm{DO} = \frac{mt - m0}{m\infty - m0} = \frac{mt\mathrm{Fe}}{m0} = \frac{\mathrm{mol}t\mathrm{Fe}}{\mathrm{mol}0}$$
$$== \frac{\mathrm{mol}tH_2\ (\text{actual hydrogen mole produced at time } t)}{\mathrm{moltotal}(\text{total hydrogen mole produced after complete oxidation})} \quad (1)$$

where $m_t$ is an actual mass of the sample at time $t$ in the oxidation stage (which was mainly composed of Fe and $Fe_3O_4$), $m_{t\mathrm{Fe}}$ the mass of the reduced sample (Fe) oxidized by $H_2O$ at time $t$, $m_0$ the initial mass of the reduced sample (Fe) fed into the reactor, $m_\infty$ the mass after complete oxidation of the reduced sample fed into reactor, $\mathrm{mol}_{t\mathrm{Fe}}$ the mole of oxidation of the reduced sample (Fe) by $H_2O$ at time $t$ and $\mathrm{mol}_0$ the initial mole of the reduced sample (Fe) fed into reactor. The values of $m_t$, $m_{tFe}$, $\mathrm{mol}_{t\mathrm{H}}$ and $\mathrm{mol}_{\mathrm{total}}$ could be obtained from experimental data.

In this work, the following equations were obtained according to step 2:

$$m_\infty - m_o = m_o \frac{1/3M\mathrm{Fe_3O_4} - M\mathrm{Fe}}{M\mathrm{Fe}} = m_o 0.3809 \quad (2)$$

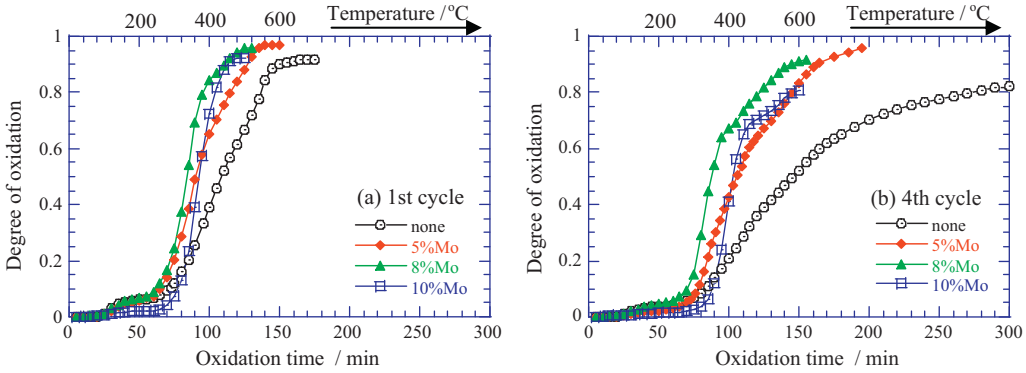


**Fig. 2.** The degree of oxidation vs. time in the reoxidation of $Fe_2O_3$-none, $Fe_2O_3$–5%Mo, $Fe_2O_3$–8%Mo and $Fe_2O_3$–10%Mo in the first and fourth redox cycles.

where $M_{Fe3O4}$ is the mol mass of $Fe_3O_4$, $M_{Fe}$ the mol mass of Fe.from Eqs. (1) and (2), the DO as a conversion ($\alpha$) also was expressed as follows:

$$\alpha = \mathrm{DO} = \frac{m_t - m_o}{m_o \times 0.3809} \tag{3}$$

### 2.4. Conventional kinetic analysis for the oxidation of the sample

A gas–solid reaction equation for step 2 can be described as

$$'aH_2O_{(g)} + bFe_{(s)} \rightarrow cH_{2(g)} + dFe_3O_{4(s)} \tag{4}$$

Accordingly, a conventional rate equation could be introduced for the oxidation of the reduced sample by $H_2O$ under isothermal conditions, which was based on the assumption of a signal-step reaction only with chemical reaction control and expressed as follow:

$$\frac{d\mathrm{mol}_{t\mathrm{Fe}}}{dt} = k \cdot P^a_{H_2O} \cdot (\mathrm{mol}_0 - \mathrm{mol}_{t\mathrm{Fe}})^b \tag{4}$$

where $a$ and $b$ represent the stoichiometric coefficients in step 2, $k$ is the rate constant and $P_{H_2O}$ is the water vapour partial pressure.

Combining Eqs. (3) and (4), a new rate equation ($d\alpha/dt$) can be obtained:

$$\frac{d\alpha}{dt} = k \cdot P^a_{H_2O} \cdot (\mathrm{mol}_0)^{b-1} \cdot (1-\alpha)^b = k \cdot P^a_{H_2O} \cdot \left(\frac{3}{4}\mathrm{mol}_{\mathrm{total}}\right)^{b-1} \cdot (1-\alpha)^b \tag{5}$$

It is seen that the $P^a_{H_2O}$ and $(\mathrm{mol}_0)^{b-1}$ in Eq. (5) are constant values due to a given $\mathrm{mol}_0$ with an invariable pressure of 20 kPa ($P_{H_2O}$) for each oxidation in isothermal conditions in this work.

$$\text{By setting } K_c = k \cdot P^a_{H_2O} \cdot (\mathrm{mol}_0)^{b-1} = k \cdot P^a_{H_2O} \cdot \left(\frac{3}{4}\mathrm{mol}_{\mathrm{total}}\right)^{b-1} \tag{6}$$

the reaction rate Eq. (5) can be simplified as:

$$\frac{d\alpha}{dt} = K_c \cdot f(\alpha) = K_c \cdot (1-\alpha)^n \tag{7}$$

where $n$ represents the so-called reaction orders in step 2, i.e., Eq. (4)′. The following equations can be obtained by integrating Eq. (7) in isothermal conditions ($\alpha \rightarrow [0,\alpha]$ and $t \rightarrow [0,t]$ interval):

$$g(\alpha) = -\ln(1-\alpha) = K_c \cdot t \quad , n = 1 \tag{8}$$

$$g(\alpha) = \frac{1-(1-\alpha)^{1-n}}{1-n} = K_c \cdot t \quad , n \neq 1 \tag{9}$$

A series of constant values of $K_c$ in isothermal conditions can be obtained by the slope of $g(\alpha)$ vs. $t$ plots based on a good linearity for an appropriate kinetic model as the criterion to determine the kinetic function $g(\alpha)$ best describing the experimental data of the oxidation process, and varying temperature from 320 to 440 °C at different temperature intervals.

The apparent activation energy of the oxidation reaction in isothermal conditions can be is introduced by replacing $k$ in Eq. (6) with the Arrhenius equation, which can be expressed as follows:

$$\ln K_c = -\frac{E_a}{RT} + \ln\left(A \cdot P^a_{H_2O} \cdot (3/4\mathrm{mol}_{\mathrm{total}})^{b-1}\right) = -\frac{E_a}{RT} + C \tag{10}$$

where $E_a$ is the apparent activation energy, $A$ the pre-exponential factor. The slope of $\ln K_c$ vs. $1/T$ can give $E_a$ of the oxidation reaction at various isothermals.

### 2.5. Jander kinetic analysis for the oxidation of the sample

A gas–solid non-catalytic reaction occurring during the oxidation of the reduced sample (Fe) by $H_2O$ has been described previously by conventional kinetic analysis. To obtain an appropriate kinetic $g(\alpha)$ function well described by the experimental data of the oxidation of Fe by $H_2O$ vapour in the isothermal conditions, a lot of kinetic models were used to investigate various gas–solid non-catalytic reactions [11–18]. Among them, the Jander equation $g(\alpha) = [1-(1-\alpha)^{0.33}]^2 = kt$, describing a three-dimensional diffusion process of a gaseous phase through a product layer [14,15], was found to be able to give a good description for the experimental data examined in isothermal conditions in this work. A set of $k$ at isothermal operating temperatures of 360, 380, 420 and 440 °C could be obtained by the slope of $[1-(1-\alpha)^{0.33}]^2$ vs. $t$ plots with high linearity, and the conversion degree ($\alpha$) versus time data for the oxidation of Fe by $H_2O$ in the range of 360–440 °C could be well fitted by Jander equation. The apparent activation energy of the oxidation reaction could be calculated by the Arrhenius equation with the rate constant $\ln k = \ln A + (-E_a/RT)$

Based on the two analysis methods stated previously, Table 1 summarizes the various kinetic models used to determine the oxidation process of the reduced samples by $H_2O$.

## 3. Results and discussion

### 3.1. Hydrogen production of the unmodified $Fe_2O_3$ and $Fe_2O_3$–(5%, 8% and 10%)Mo samples in repeated redox cycles

The changes of the rate of $H_2$ formation plotted against temperature for the unmodified $Fe_2O_3$, $Fe_2O_3$–5%Mo, $Fe_2O_3$–8%Mo and $Fe_2O_3$–10%Mo samples in four cycles are shown in Fig. 1(a–d). Comparing the kinetic curves in Fig. 1(b–d) with those in Fig. 1(a), it is obvious that the rate of $H_2$ formation of the modified samples was higher than that of the unmodified $Fe_2O_3$ sample at 300 °C and that the curves in Fig. 1(b–d) overlapped better than those in Fig. 1(a). The amount of $H_2$ production of $Fe_2O_3$–(5% and 8%)Mo in redox cycles was also larger than that of unmodified $Fe_2O_3$. These indicate that Mo cations as additive in $Fe_2O_3$ could effectively improve

**Table 1**
Expression of g($\alpha$) functions for some of reaction models based on the two kinetic analyses in gas–solid reaction.

| No. | Symbol | Reaction model | $g(\alpha)$ functions |
|---|---|---|---|
| 1 | $C_0$ | Conventional kinetics ($n=0$, zero order) | $\alpha$ |
| 2 | $C_{0.5}$ | Conventional kinetics ($n=0.5$, half-order) | $2[1-(1-\alpha)]^{1/2}$ |
| 3 | $C_1$ | Conventional kinetics ($n=1$, first order) | $-\ln(1-\alpha)$ |
| 4 | $C_{1.5}$ | Conventional kinetics ($n=1.5$, 1.5th order) | $[1-(1-\alpha)^{-1/2}]\cdot(-2)$ |
| 5 | $C_2$ | Conventional kinetics ($n=2$, 2nd order) | $(1-\alpha)^{-1/2}-1$ |
| 6 | J | Jander equation | $[1-(1-\alpha)^{1/3}]^2$ |

the activity and stability of the samples for hydrogen production in repeated redox cycles. However, the modified effects of the additive on the reoxidation of the reduced samples strongly depended on the amount of Mo cations added to the samples. It is apparent from Fig. 1(b–d) that the modified effect of $Fe_2O_3$–8%Mo was the most effective. A too big addition of Mo (10%) to $Fe_2O_3$ could cause decrease in the amount of $H_2$ production such as only the average capacity of 4.19 wt%, while a too small amount of 5%-Mo could make the oxidation time become long. The result can be observed from the changes of DO-time shown in Fig. 2(a–b). E. g., Fig. 2(a) shows that an approximate 0.80 DO could be achieved in less than 90 min for the re-oxidation of the reduced $Fe_2O_3$–8%Mo sample in the first cycle, but to obtain the same DO for the $Fe_2O_3$–5%Mo and $Fe_2O_3$–10%Mo samples were not less than 100 and 110 min, respectively. From the comparisons of the kinetic curves for the unmodified $Fe_2O_3$, $Fe_2O_3$–5%Mo, $Fe_2O_3$–8%Mo and $Fe_2O_3$–10%Mo sample in the first and fourth cycles shown in Fig. 2(a–b), it is obvious that the order of the DO was $Fe_2O_3$–8%Mo > $Fe_2O_3$–5%Mo, $Fe_2O_3$–10%Mo > unmodified $Fe_2O_3$, within the same reaction time. It concluded that $Fe_2O_3$–8%Mo was the most effective for increasing the formation rate of $H_2$ and decreasing the temperature of $H_2$ formation among all the samples.

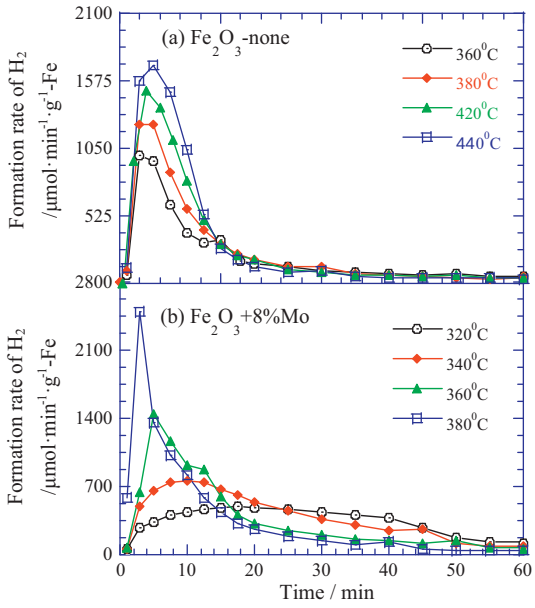


**Fig. 3.** The formation rate of $H_2$ vs. time curves for the oxidation of the reduced samples at isothermal temperatures of 360, 380, 420 and 440 °C for $Fe_2O_3$-none and of 320, 340, 360 and 380 °C for $Fe_2O_3$–8%Mo.

### 3.2. Isothermal kinetic results of the unmodified $Fe_2O_3$ and $Fe_2O_3$–8%Mo samples

The kinetic studies on the oxidation process of unmodified $Fe_2O_3$ and $Fe_2O_3$–8%Mo in the redox cycle were carried out at different isothermal operating temperatures. To determine an appropriate reaction model for the oxidation of the reduced sample by $H_2O$ in this work, two kinds of the kinetic analysis methods have been previously proposed to expect to well be described by the experimental data of isothermal kinetics. The isothermal kinetic curves of oxidation of the reduced samples for unmodified $Fe_2O_3$ in the range of 360–440 °C and for $Fe_2O_3$–8%Mo in the range of 320–380 °C are given in Fig. 3. The changes of DO vs. time are given in Fig. 4. The DO in Fig. 4 was obtained by Eq. (5) based on the integrated area under the curves in Fig. 3. According to the results of Fig. 4, i.e. the $\alpha$ values at time $t$, Figs. 5 and 6 were plotted by the conventional kinetic and Jander models, respectively.

Fig. 5(a–d) and (a′–d′) shows the changes of the function g(α) in Eqs. (8) and (9) vs. time for $b=0.5$, 1, 1.5 and 2, respectively. It is apparent from Fig. 5 that a relatively higher linearity of $\frac{1-(1-\alpha)^{1-n}}{1-n}$ vs. $t$ plot was observed in Fig. 5(c) and (c′) when the reaction order was assumed as $n=1.5$. This result indicates that the oxidation of the reduced unmodified $Fe_2O_3$ or $Fe_2O_3$-8%Mo sample by $H_2O$ vapour in Eq. (6)′ was a gas-solid oxidation reaction with the 1.5th order and can be explained by the conventional kinetic models. The apparent activation energies of the oxidation reaction obtained by fitting the experimental data summarized in Table 2 are 65.30 kJ mol$^{-1}$ for unmodified $Fe_2O_3$ and 45.19 kJ mol$^{-1}$ for $Fe_2O_3$–8%Mo. This result will be subsequently supported by Jander equation below.

Fig. 6 (a–b) shows the changes of the function g(α) vs. time by Jander equation $g(\alpha)=[1-(1-\alpha)^{0.33}]^2=kt$. It is clear that the linearity of the plot of $[1-(1-\alpha)^{0.33}]^2$ vs. time decreases with increasing isothermal operating temperature. Although being in the case, the Jander equation still gave the best description. The apparent activation energies of the oxidation reaction listed in Table 3 are given by the equations of $\ln k=2.8381-6679\,T^{-1}$ and $\ln k=0.9425-4351\,T^{-1}$, which are 55.53 kJ mol$^{-1}$ for unmodified $Fe_2O_3$ and 36.17 kJ mol$^{-1}$ for $Fe_2O_3$–8%Mo, and the frequency factor $A=17.08$ and 2.57 min$^{-1}$, respectively. The two values are close to the activation energies (65.30 and 45.19 kJ mol$^{-1}$) previously described by conventional kinetic model, indicating that the Jander equation describes the oxidation process of the reaction adequately.

It is obvious that the two kinetic models can give the good description of the experimental data examined in the present work. The apparent activation energy of the oxidation reaction for unmodified $Fe_2O_3$ is in the range of about 55.53–65.30 kJ mol$^{-1}$

**Table 2**
Kinetic parameters based on g(a) function expressions by the conventional kinetics.

| Sample | $n$ | $g(\alpha)$ functions | $E_a$ (kJ/mol) | Corr. coeff |
|---|---|---|---|---|
| $Fe_2O_3$-none | 0 | $\alpha$ | – | – |
| | 0.5 | $2[1-(1-\alpha)]^{1/2}$ | – | – |
| | 1 | $-\ln(1-\alpha)$ | 40.61 | 0.9659 |
| | 1.5 | $[1-(1-\alpha)^{-1/2}]\cdot(-2)$ | 65.30 | 0.9909 |
| | 2 | $(1-\alpha)^{-1/2}-1$ | 93.67 | 0.9531 |
| $Fe_2O_3$–8%Mo | 0 | $\alpha$ | – | – |
| | 0.5 | $2[1-(1-\alpha)]^{1/2}$ | – | – |
| | 1 | $-\ln(1-\alpha)$ | 31.63 | 0.9788 |
| | 1.5 | $[1-(1-\alpha)^{-1/2}]\cdot(-2)$ | 45.19 | 0.9986 |
| | 2 | $(1-\alpha)^{-1/2}-1$ | 60.31 | 0.9538 |

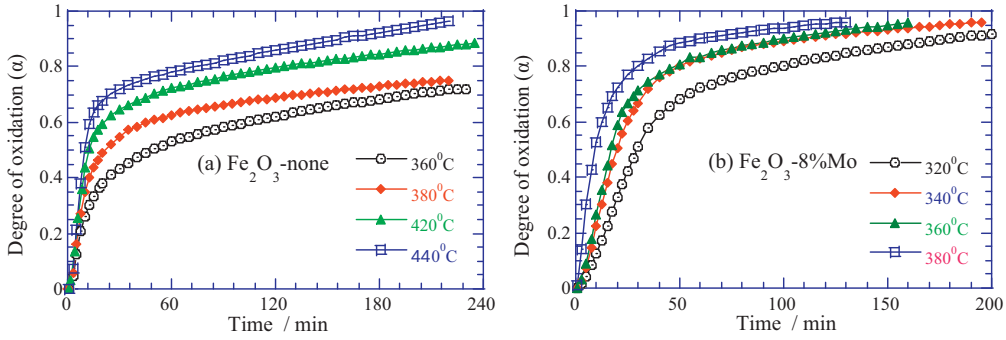


**Fig. 4.** The degree of oxidation ($\alpha$) vs. time curves for the oxidation of the reduced samples at isothermal temperatures of 360, 380, 420 and 440 °C for $Fe_2O_3$-none and of 320, 340, 360 and 380 °C for $Fe_2O_3$–8%Mo.

and for $Fe_2O_3$–8%Mo in the range of about 36.17–45.19 kJ mol$^{-1}$. The oxidation process for both samples is suitable for a gas–solid non-catalytic reaction with the 1.5th order described by the conventional kinetics model and a three-dimensional diffusion reaction of a gaseous phase through a product layer described by Jander kinetics model. In addition, the lower apparent activation energy of $Fe_2O_3$–8%Mo than that of unmodified $Fe_2O_3$ showed the effective modification effect of Mo cations added to the sample.

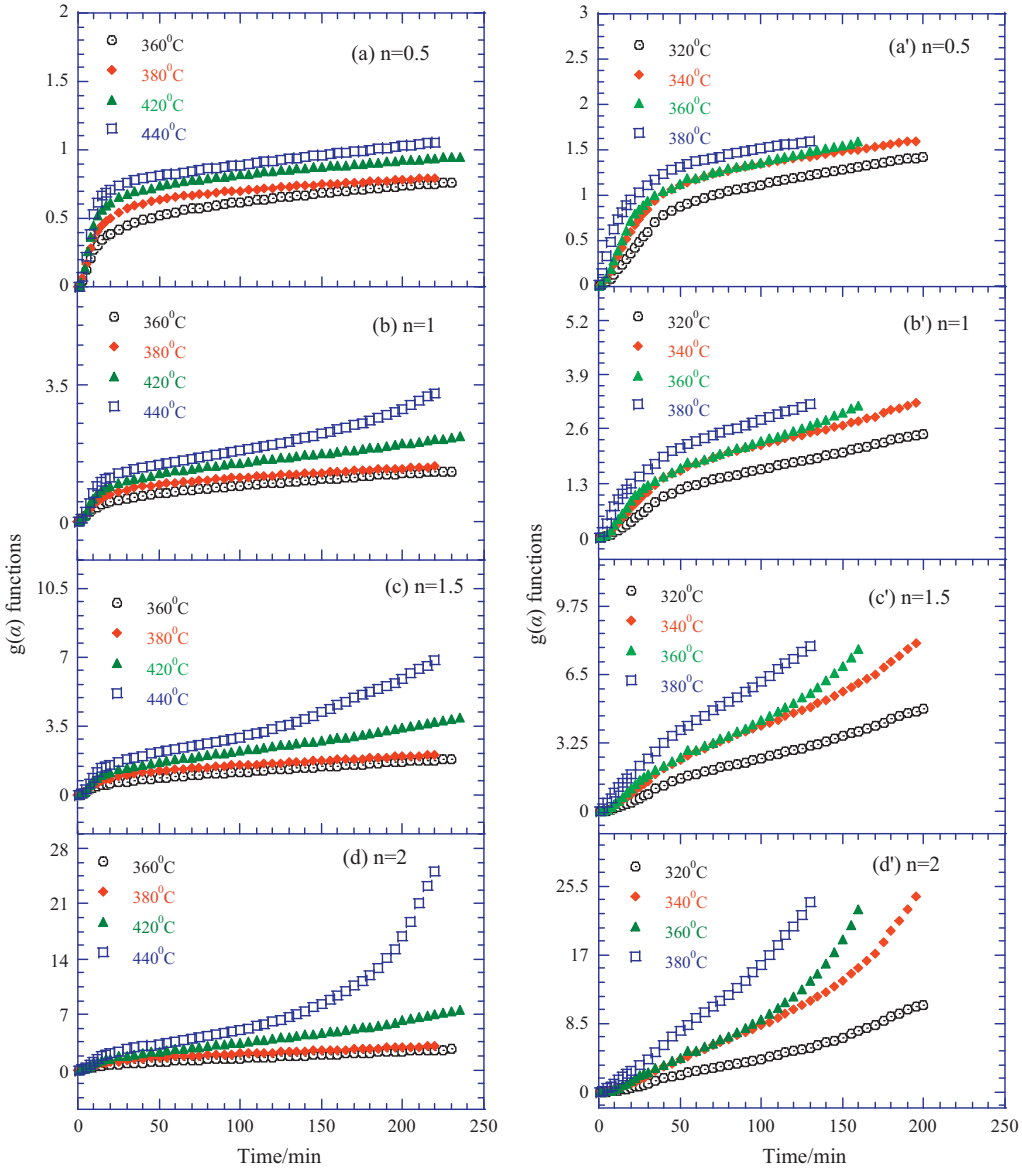


**Fig. 5.** Determination of the reaction model based on the conventional kinetic analysis for $Fe_2O_3$-none and $Fe_2O_3$–8%Mo; $g(\alpha)=2[1-(1-\alpha)]^{1/2}$, $-\ln(1-\alpha)$, $[1-(1-\alpha)^{-1/2}]\cdot(-2)$ and $(1-\alpha)^{-1/2}-1$ at $n=0.5$, 1, 1.5 and 2, respectively.

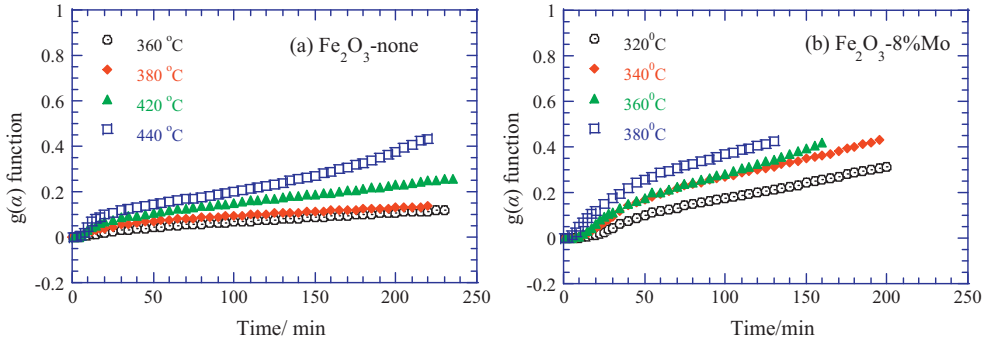


**Fig. 6.** Plots of $g(\alpha)$ vs. time by Jander equation; $g(\alpha) = [1-(1-\alpha)^{1/3}]^2$.

**Table 3**
Kinetic parameters for the oxidation of the reduced sample by the Jander equation.

| Sample | Temp (°C) | $k$ | Corr. coeff. | $\ln k$ | $1/T$ | $E_a$ (kJ/mol) |
|---|---|---|---|---|---|---|
| $Fe_2O_3$-none | 360 | $4.951 \times 10^{-4}$ | 0.9983 | −7.6108 | 0.001579 | 55.53 |
| | 380 | $5.553 \times 10^{-4}$ | 0.9952 | −7.4960 | 0.001531 | |
| | 420 | $9.842 \times 10^{-4}$ | 0.9854 | −6.9237 | 0.001443 | |
| | 440 | $1.649 \times 10^{-3}$ | 0.9569 | −6.4075 | 0.001402 | |
| $Fe_2O_3$–8%Mo | 320 | $1.632 \times 10^{-3}$ | 0.9929 | −6.4179 | 0.001686 | 36.17 |
| | 340 | $2.219 \times 10^{-3}$ | 0.9877 | −6.1109 | 0.001631 | |
| | 360 | $2.611 \times 10^{-3}$ | 0.9817 | −5.9481 | 0.00158 | |
| | 380 | $3.265 \times 10^{-3}$ | 0.9703 | −5.7245 | 0.001531 | |

The reason for it may be that the cooperative effect of active Fe and Mo additive on the $H_2O$ decomposition changes the original path of the oxidation reaction, which needs to be further confirmed in the next work. This was also mainly the reason why $Fe_2O_3$–8%Mo has a higher rate of $H_2$ formation and a lower temperature of $H_2$ formation than unmodified $Fe_2O_3$.

## 4. Conclusion

Summarily, the unmodified $Fe_2O_3$, $Fe_2O_3$–5%Mo, $Fe_2O_3$–8%Mo and $Fe_2O_3$–10%Mo samples were prepared by hydrothermal synthesis. The effects of various amounts of Mo cations on the hydrogen production of the samples were investigated. The kinetic studies on the oxidation process of unmodified $Fe_2O_3$ and $Fe_2O_3$–8%Mo were also carried out at different isothermal operating temperatures. The results show that $Fe_2O_3$–8%Mo was the most effective for enhancing the $H_2$ forming rate at low temperatures (<300 °C) and decreasing the $H_2$ forming temperature. The apparent activation energy of the oxidation process was about 55.53–65.30 kJ mol$^{-1}$ for unmodified $Fe_2O_3$ and about 36.17–45.19 kJ mol$^{-1}$ for $Fe_2O_3$–8%Mo based on the conventional and Jander models. The lower apparent activation energy of $Fe_2O_3$–8%Mo than that of unmodified $Fe_2O_3$ showed the effective modification effect of Mo cations added to the sample.

## Acknowledgements

The authors acknowledge the financial supports of the National Hi-Tech Research and Development Program (863) of China (no. 2007AA05Z116), the National Natural Science Foundation of China (no. 20873099, 20673082), the Scientific Research Foundation for ROCS, SEM. (no. 2006331), the Key Project of Science and Technology of Shaanxi Province (no.2005k07-G2), and the Natural Science Foundation of Shaanxi education Committee (no.06JK167). The authors are also grateful to the State Key Laboratory of Continental Dynamics for the SEM measurements.

## References

[1] W. Grochala, P.P. Edwards, Thermal decomposition of the non-interstitial hydrides for the storage and production of hydrogen, Chem. Rev. 104 (2004) 1283–1316.
[2] P. Kruger, Electric power requirement for large-scale production of hydrogen fuel for the world vehicle fleet, Int. J. Hydrogen Energy 26 (2001) 1137–1147.
[3] J.A. Peña, E. Lorente, E. Romero, Kinetic study of the redox process for storing hydrogen: reduction stage, J. Herguido Catal. Today 116 (2006) 439–444.
[4] G.H. Lara, G. Momen, P.H. Marty, B.L. Neindre, K. Hassouni, Hydrogen storage by adsorption on activated carbon: Investigation of the thermal effects during the charging process, Int. J. Hydrogen Energy 32 (2007) 1542–1553.
[5] K. Otsuka, T. Kaburagi, C. Yamada, S. Takenaka, Chemical storage of hydrogen by modified iron oxides, J. Power Sources 122 (2003) 111–121.
[6] K. Otsuka, C. Yamada, T. Kaburagi, S. Takenaka, Hydrogen storage and production by redox of iron oxide for polymer electrolyte fuel cell vehicles, Int. J. Hydrogen Energy 28 (2003) 335–342.
[7] H. Wang, S. Takenaka, K. Otsuka, Hydrogen storage properties of modified fumed-Fe-dust generated from a revolving furnace at a steel industry, Int. J. Hydrogen Energy 31 (2006) 1732–1746.
[8] H. Wang, G. Wang, X.Z. Wang, J.B. Bai, Hydrogen production by redox of cation-modified iron oxide, J. Phys. Chem. C 112 (2008) 5679–5688.
[9] H. Wang, X.Q. Feng, X.F. Wang, S.P. Cheng, S.L. Gao, Hydrogen production by redox of bimetal cation-modified iron oxide, Int. J. Hydrogen Energy 33 (2008) 7122–7128.
[10] J.C. Ryu, D.H. Lee, K.S. Kang, C.S. Park, J.W. Kim, Y.H. Kim, Effect of additives on redox behavior of iron oxide for chemical hydrogen storage, J. Ind. Eng. Chem. 14 (2008) 252–260.
[11] W.K. Jozwiak, E. Kaczmarek, T.P. Maniecki, W. Ignaczak, W. Maniukiewicz, Reduction behavior of iron oxides in hydrogen and carbon monoxide atmospheres, Appl. Catal. A Gen. 326 (2007) 17–27.
[12] M.J. Tiernan, P.A. Barnes, G.M.B. Parkes, Reduction of iron oxide catalysts: the investigation of kinetic parameters using rate perturbation and linear heating thermoanalytical techniques, J. Phys. Chem. B 105 (2001) 220–228.
[13] D.B. Bukur, K. Okabe, M.P. Rosynek, C. Li, D. Wang, K.R.P.M. Rao, G.P. Huffman, Activation studies with a precipitated iron catalyst for fischer-tropsch synthesis: I. characterization studies, J. Catal. 155 (1995) 353–365.
[14] B. Jankovic, Isothermal reduction kinetics of nickel oxide using hydrogen: conventional and weibull kinetic analysis, J. Phys. Chem. Solids 68 (2007) 2233–2246.
[15] C.P.J. van Vuuren, P.P. Stander, The oxidation kinetics of $FeV_2O_4$ in the range 200–500 °C, Thermochim. Acta 254 (1995) 227–233.
[16] P. Meakin, Simulation of the effects of fractal geometry on the selectivity of heterogeneous catalysts, Chem. Phys. Lett. 123 (1986) 428–432.
[17] A.P. Grosvenor, B.A. Kobe, N.S. McIntyre, Studies of the oxidation of iron by water vapour using X-ray photoelectron spectroscopy and QUASES™, Surf. Sci. 572 (2004) 217–227.
[18] I. Hironori, M. Akira, M. Takeyuki, M. Shigeru, A. Takashi, Effects of reduction conditions on the cycling performance of hydrogen storage by iron oxides: storage stage, Chem. Eng. Sci. 63 (2008) 4974–4980.